J Mater Sci (2019) 54:5813–5824

Metals

An improved method for the matrix dissolution extraction of nanoparticles from microalloyed steel

Andreas Hegetschweiler[1], Thorsten Staudt[2], and Tobias Kraus[1,3,*]

[1] *INM - Leibniz Institute for New Materials, Campus D2 2, 66123 Saarbrücken, Germany*
[2] *AG der Dillinger Hüttenwerke, Werkstraße 1, 66763 Dillingen/Saar, Germany*
[3] *Colloid and Interface Chemistry, Saarland University, Campus D2 2, 66123 Saarbrücken, Germany*

Received: 1 August 2018
Accepted: 14 December 2018
Published online: 2 January 2019

ABSTRACT

The chemical extraction of niobium and titanium carbonitride precipitates from microalloyed steels was studied. Steel samples and chemically synthesized reference nanoparticles were subjected to commonly used extraction protocols, and conditions were systematically varied. High acid concentrations led to particle etching with losses above 10%; long extraction times and small etchant volumes led to the formation of dense SiO_x networks that engulfed the extracted particles. The addition of surfactants was found to reduce agglomeration and limit etching. We developed an optimized extraction protocol that can extract and retain particles with diameters below 10 nm with reduced etching and negligible network formation. The resulting particle dispersions are suitable both for efficient electron microscopy of large particle numbers in a single run and colloidal analysis of large numbers of particles in dispersion.

Introduction

Microalloyed, thermomechanically rolled steels are widely used for pipeline and offshore construction. They surpass regular carbon steels in mechanical properties but retain good weldability. Microalloyed steels contain small amounts of niobium, titanium, and/or vanadium that precipitate during the thermomechanical controlled rolling process (TMCP) as carbide, nitride, and/or carbonitride particles. The precipitates affect the microstructure depending on their size and precipitation timing; some of them improve the steel properties. Particles that precipitate at high temperatures can pin grain boundaries, thus preventing austenite grain growth at early stages of the TMCP. There were different sizes reported for these particles; they range from around 20 nm [1] to roughly 300 nm [2] depending on the processing conditions. Particles that precipitate during hot rolling usually have diameters between 10 and 100 nm. They form in highly deformed grains and retard recrystallization, leading to a highly deformed microstructure with a high dislocation density at the austenite–ferrite transition. The dislocations nucleate ferrite grains so that a high particle density leads to a fine ferrite grain structure. Particles that precipitate at the end of the process during cooling have typical

Address correspondence to E-mail: tobias.kraus@leibniz-inm.de

https://doi.org/10.1007/s10853-018-03263-0

diameters below 10 nm and improve the mechanical strength by precipitation hardening [2–4].

Advanced steel process development requires the knowledge of the particle size and composition distributions. For example, an efficient use of the microalloying elements requires information on the time-dependent particle size distribution (PSD) that indicates whether the microalloying elements precipitate during the expected stage of TMCP and can thus influence the microstructure as desired. Today, particles in steel are mostly analyzed using transmission electron microscopy (TEM) of electron transparent foils or carbon extraction replicas [5–13]. Modern electron microscopy provides enough resolution even for the smallest particles of interest and provides additional insights in the structure of individual particles. Elemental analysis with energy-dispersive X-Ray analysis (EDX) or electron energy loss spectroscopy (EELS) provides the composition of single particles. However, the steel matrix in electron transparent foils impedes composition analysis and affects the measurement with its magnetism. Preparation of carbon extraction replicas may incur unwanted particle etching, and the extraction efficiency can be different for different sized particles [14]. The number of particles that can be observed in one electron micrograph is typically limited to 100–1000 [11, 15]. Common particle analysis procedures for electron microscopy recommend analyzing at least 400–500 nanoparticles [16, 17]; reliable statistical statements on complex PSD routinely require more than 10^4 particles [18].

Matrix dissolution extraction is a fundamentally different approach for the analysis of particles in steel. Originally conceived before electron microscopy became available, the method is based on the chemical [19] or electrolytic [20] removal of the matrix. Chemical etchants such as hydrochloric acid or halogens oxidize and dissolve the iron such that the particles remain as a solid residue. The method has been successfully applied for many steels [19, 21–23], including microalloyed steels that contain Nb and Ti-carbonitride nanoparticles [24–27]. It gives access to particles from a much larger sample volume than carbon extraction replicas or TEM foils, and the extracted particles can be investigated by electron microscopy, X-ray diffraction (XRD), or elementary analysis methods such as mass spectrometry or optical emission spectroscopy with inductively coupled plasma (ICP-MS or ICP-OES) [25, 28, 29]. Matrix dissolution provides much higher particle concentrations than in the original steel and removes cementite and other particles that can be mistaken for inclusions, but the information on the original particle configuration is lost. It simplifies X-ray diffraction analysis with Rietveld refinement [25, 28]. Elementary analysis provides particle composition and allows the researcher to calculate the precipitation efficiency of the microalloying elements [25, 29]. Thus, matrix dissolution in combination with particle analysis is particularly useful to optimize alloy composition and the processing parameters of the TMCP.

Three major problems currently limit the usefulness of particle extraction for the analysis of small particles in steel: SiO_x network formation, etching of the extracted particles, and agglomeration of the extracted particles. Most existing protocols, including the ASTM Standard E 194-10 [30], use acids that lead to SiO_x network formation when applied to silicon-containing steels. Lu et al. [25] reported difficulties in electron microscopy and an amorphous signal in the diffractogram when they extracted Nb and Ti-carbonitride particles from microalloyed steels. Unwanted etching of the extracted particles was not considered because the carbides, nitrides, and carbonitrides of microalloy elements were expected to be chemically stable in diluted inorganic acids at room temperature [31–35]. However, small particles often differ from bulk materials in their chemical behavior. Finally, agglomeration of the particles may impede the successful characterization of the extracted particles, for example, in the automated image analysis of TEM/SEM micrographs.

This study seeks matrix dissolution protocols that minimize SiO_x network formation, particle etching, and agglomeration. A microalloyed steel (Grade X100) was selected as representative target material. It contained Nb, Ti, V, Si, Mn, N, and Cr as alloy elements that may interact with the extraction reagents and influence the extraction process. Copper, Ni, and Mo were not alloyed. This steel is known to form Nb, Ti, and NbTi-carbonitrides with different sizes and compositions during different phases of the thermomechanical processing that cause grain refinement and precipitation hardening. All Nb and Ti in the steel samples were therefore contained in particles. Vanadium, by contrast, remained in solid solution, because Nb and Ti precipitate first and deplete C and N that are necessary for V carbonitride

precipitation. Vanadium-containing particles were therefore not expected to occur. Niobium and Ti in the etching solution could only be present due to unwanted etching of the target particles. We used this situation to study whether the extracted Nb and Ti carbonitride particles had been etched and whether elements in solution (such as silicon) somehow affected extraction.

Samples were dissolved using different and systematically varied protocols and the results were quantified. We found no V-containing precipitates and considerable etching of Nb and Ti-carbonitrides when using standard protocols. An improved protocol based on sulfuric acid at a concentration of 0.5 mol L^{-1}, increased centrifugation time, and the addition of a dispersant led to reduced etching of 11% for Nb and 18% for Ti and improved the yield for particles with diameters below 10 nm.

Experimental procedures

Materials

A microalloyed thermomechanically rolled pipeline steel (Grade X100) with the composition given in Table 1 was used as representative steel sample that contains both Nb and Ti. Samples of 1 g of steel chippings were dissolved in different volumes of hydrochloric acid (HCl) at 6 mol L^{-1} and sulfuric acid (H_2SO_4) at 0.5 mol L^{-1} and 2 mol L^{-1}, respectively. The etching solutions were freshly prepared from concentrated HCl (Carl Roth, 37%, p.a., Germany) and concentrated H_2SO_4 (Sigma-Aldrich, 95–97%, p.a., Germany) by diluting with ultrapure water. A dispersant (Disperbyk-2012, Byk, Germany) was added in some of the samples (see "Extraction procedure" section).

The digestion acid mixture used to dissolve the extracted particles for elemental analysis was composed of 25 mL concentrated HCl (Sigma Aldrich, ≥ 37%, puriss p.a., Germany), 8 mL concentrated nitric acid (Sigma Aldrich, ≥ 65%, puriss. p.a., Germany), and 17 mL ultrapure water.

Niobium and Ti-carbonitride reference particles were synthesized according to Giordano et al. [36]. $TiCl_4$ or $NbCl_5$ was dissolved in ethanol together with urea and then subjected to a heat treatment at approx. 800 °C under N_2 atmosphere for several hours. The particles had diameters according to TEM (approx. 100 particles measured) between 10 and 50 nm in a partially aggregated state.

Characterization methods

Electron microscopy was performed using a JEM 2100 transmission electron microscope (TEM) (JEOL, Germany) with an acceleration voltage of 200 kV. For sample preparation, 2.5 µL of the sample solution was dried on a copper TEM grid with a carbon film. Image analysis was performed with *DigitalMicrograph*^{TM} from Gatan, Inc.

Inductively coupled plasma optical emission spectroscopy (ICP-OES) analysis was performed using an Ultima 2 spectrometer (Horiba Jobin–Yvon, Germany). The supernatant was atomized without any further treatment. To analyze the elementary composition of the particles, 5 mL of the digestion acid mixture (see above) was added to the iron-free particle dispersion (5 mL). The mixture was transferred to a Teflon microwave container containing 1 mL of hydrofluoric acid (Riedel-de Haën, 50%, p.a. plus, Germany), exposed to microwave irradiation (0 to 800 W ramp in 60 min, constant 800 W for 90 min) in a pressure vessel (p_{max} = 60 bar), filled to 50 mL with ultrapure water, and analyzed.

All measurements were taken on two aliquots drawn from the original dissolved sample, and the average of both measurements is reported here. Errors were calculated for both aliquots using standard error propagation based on the standard deviation of 9 ICP-OES measurements and estimated volume errors from pipetting, and the larger of the two errors are shown as error bars in all graphs. Errors due to particle loss in centrifugation were not considered and explain the difference to 100% recovery.

Table 1 Elemental composition of the examined steel. Cu, Ni, and Mo are not alloyed

Element	C	Si	Mn	N	Cr	V	Nb	Ti	CEV[a]
Wt%	0.07	0.35	1.9	0.003	0.2	0.04	0.05	0.02	0.44

[a]*CEV* carbon equivalent value

Extraction procedure

Microalloyed steel

The first matrix dissolution protocol was based on the ASTM standard E 194-10[1]: 1 g of steel chippings was added to 20 mL HCl with a concentration of 6 mol L^{-1} at room temperature. When the sample had been fully dissolved, the solution was heated to boil. 30 mL of water was added and heated to boil again. The protocol was then systematically varied: 1 g of sample was added to 50 mL of each of 6 mol L^{-1} HCl, 2 mol L^{-1} H_2SO_4, 0.5 mol L^{-1} H_2SO_4, and 0.5 mol L^{-1} H_2SO_4 and 0.1 vol% Disperbyk-2012. One additional sample was dissolved with 200 mL of 0.5 mol L^{-1} H_2SO_4. All etching solutions were heated to 70 °C in an oil bath and stirred at 200 rpm until the sample had been dissolved. We deviated from the ASTM standard procedure for all but the first protocol and did not boil the solution or add water.

After dissolution, all samples were sonicated for 1 min in an ultrasonic bath (Elma X-tra 50 H, 160 W, Germany). To remove the dissolved iron, each particle suspension was split in two 25 mL aliquots and centrifuged in an ultracentrifuge (XL-I 70 K, Beckman-Coulter, Germany) at 113.000 rcf and 20 °C for 120 min (180 min for the sample with surfactant). After the first run, the supernatant (20 mL) was removed for elemental analysis by ICP-OES. Seven more centrifugation steps were necessary to remove the dissolved iron to below 5×10^{-3} mmol L^{-1} and obtain a suspension of the extracted particles in water.

Reference particles

Particle etching was also tested using well-defined reference particles. An amount of 0.23 mg TiCN or 0.55 mg NbCN reference particles was treated in analogy to ASTM E 194-10 and placed in a glass beaker with 20 mL HCl at 6 mol L^{-1}. Samples of 0.5 mL were taken after 1 h, 2 h, 4 h, 8 h, and 24 h, placed in a centrifugal filter (10 kDa, Pall), and centrifuged (Centrifuge 5418, Eppendorf, Germany) at 16.873 rcf for 10 min. The particle-free liquid was then analyzed for dissolved elements using ICP-OES. After 24 h, the particle dispersion was heated to boil as per ASTM protocol, 30 mL of water was added, and the mixture was again heated to boil. A final sample was taken and treated as above.

The same amounts of reference particles were also subjected to the modified dissolution protocols. Particles were added to the acid mixture in question and sonicated for 1 min. The dispersions were placed in an oil bath and heated under reflux while stirring at 200 rpm. Samples of 0.5 mL were taken after 1 h, 2 h, 4 h, 8 h, and 24 h, centrifuged, and analyzed as above.

[1] The standard uses 5 g of steel that are dissolved in 100 mL HCl (6 mol L^{-1}) and later filled up with 150 mL water.

Results

Particle etching

Microalloyed steel

The times required to dissolve the steel samples varied strongly depending on the chosen protocol. The ASTM protocol dissolved 1 g in 3 days in 20 mL at room temperature. Increasing the temperature to 70 °C, increasing the liquid volume to 50 mL, and increasing acid concentration decreased the time: a sample was dissolved after 100 min in 6 mol L^{-1} HCl, after 180 min in 2 mol L^{-1} H_2SO_4, and after 460 min in 0.5 mol L^{-1} H_2SO_4. A further increase in etchant volume at constant acid solution concentration did not reduce the time required.

We found dissolved Ti and Nb in the supernatants for all protocols, with amounts that depended strongly on the protocol. Figure 1a shows the amount of Ti in the supernatant after the first centrifugation as a fraction of the total amount of alloyed Ti. The extraction yield was calculated as the fraction of Ti in the extraction residue of the total amount of alloyed Ti after the final 8th centrifugation run. Note that the dissolved elements could originate either from unwanted etching of the extracted particles or could be released from solid solution in the steel matrix (see "Particle etching" section).

The supernatant contained approximately 9% of the total Ti for samples dissolved using the ASTM protocol at a particle extraction yield of 75%. Increasing temperature and acid volume did not much affect the Ti content of the supernatant (6%) or the extraction yield (75%). However, replacing 6 mol L^{-1} HCl by H_2SO_4 increased the dissolved Ti to 19% for 2 mol L^{-1} H_2SO_4 and 18% for the 0.5 mol L^{-1} H_2SO_4, respectively, at extraction yields of

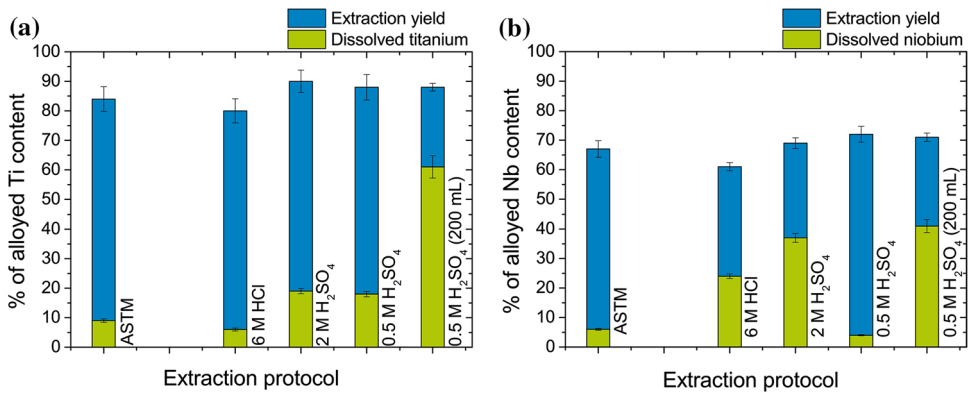

Figure 1 Concentrations of **a** titanium and **b** niobium in the supernatant (green) after the first centrifugation run and extraction yield (blue) of both elements after the 8th centrifugation for different extraction procedures. The values refer to the total alloy content of Ti or Nb in the steel.

approximately 70% for both. Increasing the acid volume further increased the amount of dissolved Ti.

The ASTM protocol led to 6% dissolved Nb at an extraction yield of 66% (Fig. 1b). Increasing the volume and temperature strongly increased the Nb amount in solution. Extraction with 6 mol L^{-1} HCl at 70 °C led to 24% dissolved Nb at an extraction yield of 33%. Sample dissolution with 2 mol L^{-1} H_2SO_4 led to 35% dissolved Nb and 32% in the residue; the dissolved amount at 0.5 mol L^{-1} was only 4%, with 68% in the residue. Increasing the acid volume markedly increased the Nb concentration in the supernatant and decreased it in the extraction yield.

In summary, more than 6% of Ti and more than 4% of Nb were found in the supernatants for all protocols. We believe that a large fraction of this quantity originated from unwanted particle etching during extraction, and only a smaller part originates directly from solid solution. The etching of reference particles was studied to verify this hypothesis and better quantify the extent of particle etching.

Reference particles

Reference particles allowed analyzing unwanted etching of TiCN and NbCN without the iron matrix. The results clearly indicated particle etching for all protocols. Figure 2 shows the release of dissolved Ti and Nb from Ti or Nb-carbonitride reference particles as the ratio of Ti or Nb found in the supernatant to the total amount of Ti or Nb in the particles.

The etching of TiCN particles in the ASTM protocol was steady but particularly severe during the boiling step after 24 h, where up to 77% of the particles were dissolved. Modified protocols with dissolution at an increased temperature of 70 °C led to similar trends: strong etching in the first hour, then saturation at Ti levels at or below those found for ASTM. Increasing the acid volume increased Ti loss.

The etching of NbCN particles strongly depended on the etching solution. The loss of Nb during the ASTM protocol was minor before boiling and reached 16% after its completion. All other etchants caused greater losses, and some of them were prohibitive: 6 mol L^{-1} HCl dissolved 76% after a rapid initial phase and a slow but steady etching; the trend was similar for 2 mol L^{-1} H_2SO_4 at a somewhat lower loss level that reached 72%. More useful was 0.5 mol L^{-1} H_2SO_4 with 18% loss. The volume of etchant had little effect on the total particle loss.

SiO_x network formation

Typical microalloyed steels contain 0.2–0.4 wt% silicon to stabilize the ferrite phase and for solution strengthening. During extraction, silicon partially dissolves and forms gel-like networks that impede analysis [24, 37]. The silicon content in the supernatant as a fraction of the steels' content depended on the extraction procedure (Fig. 3).

Sample dissolution following ASTM led to 15% silicon in the supernatant and 47% in the residue. Extraction at higher temperatures generally led to much more silicon in the supernatant and less in the residue; at 6 mol L^{-1} HCl 61% were found in the supernatant and only 2% in the residue. Sulfuric acid led to similar results for both concentrations and volumes.

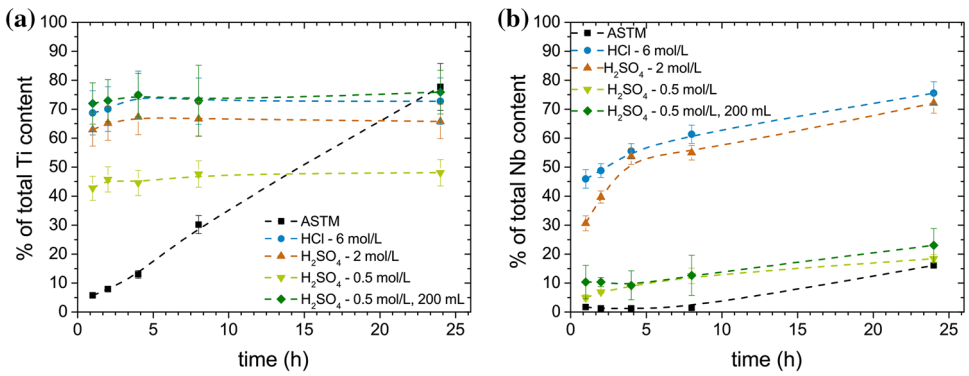

Figure 2 Time-dependent dissolution of **a** titanium and **b** niobium reference particles in different etching solutions. The values refer to the total amount of Ti and Nb in the reference particles.

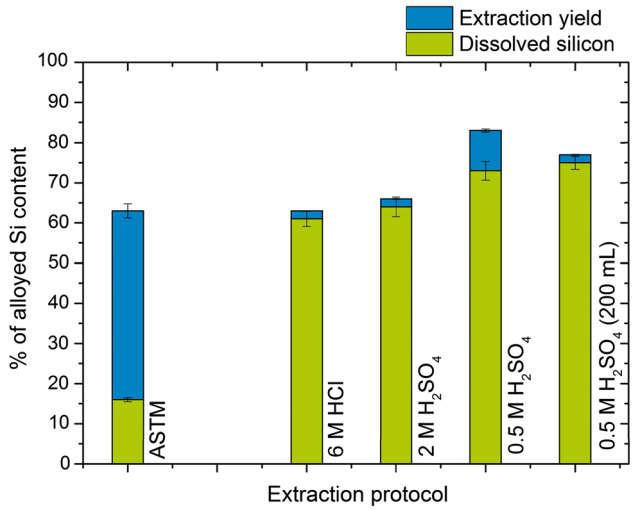

Figure 3 Silicon content based on the total amount of alloyed silicon in the supernatant (green) and in the extraction yield (blue) depending on the extraction procedure.

Dispersant

A stable colloidal dispersion of the extracted particles is desirable, but the large ionic strength of the dissolved iron and the low pH of the etchants tend to cause agglomeration. We tested surfactants to prevent destabilization and found that surface-active additives also reduced SiO_x network formation and reduced etching (Fig. 4).

The SiO_x network that formed during the ASTM protocol engulfed all particles, and particle analysis was strongly influenced (Fig. 4a). Extraction with 6 mol L^{-1} HCl (Fig. 4b) and 2 mol L^{-1} H_2SO_4 (Fig. 4c) at 70 °C reduced SiO_x network formation such that most large particles remained dispersed, but particles below approximately 50 nm were trapped in SiO_x. Extraction with 0.5 mol L^{-1} H_2SO_4 at 70 °C increased SiO_x network formation (Fig. 4d). The optimal situation was reached when using 0.5 mol L^{-1} H_2SO_4 and 0.1 vol% of the commercial surfactant mixture Disperbyk-2012 that is based on a block copolymer (Fig. 4e, f). No SiO_x network is visible, only the surfactant causes shadows (Fig. 4e) and coats the particles (Fig. 4f).

Energy-dispersive X-ray (EDX) analysis of the extracted particles confirmed that the Si content in the residues decreased for the modified protocols and the particles extracted exclusively contained Nb and Ti carbides, nitrides, and carbonitrides. Extraction according to ASTM standard led to extensive silica networks (Fig. 4a, g) with embedded particles. The improved protocols yielded dispersions that mainly contained Nb and Ti-based particles; other elements such as V or Cr (that may originate from the TEM sample holder), Cu (that may originate from the TEM grid), Al, and Fe (see Fig. 4h, i) were only found in traces.

Surfactant addition affected particle etching and extraction yield, too. Supernatants after the first centrifugation run and residues after 8 centrifugation cycles were analyzed regarding their Ti, Nb, and silicon content (Fig. 5a–c). The loss of Ti remained unchanged upon surfactant addition, while the Nb content in the supernatant was increased to 25% and the yield decreased to 37%. The silicon content in the residue was clearly decreased to only 1%. Increasing the centrifugation time (Fig. 5d) from 3 to 8 h marginally decreased the dissolved Nb to 24% but increased the extraction yield to 53%. Further increase in the centrifugation time led to a decrease in Nb in the supernatant to only 11% and to an extraction yield of 60%. The amounts of Ti in the supernatant and in the extraction yield were not affected by a longer centrifugation time.

Adding a dispersant reduced particle etching (Fig. 6), and its effect was greatest during the initial stages of extraction.

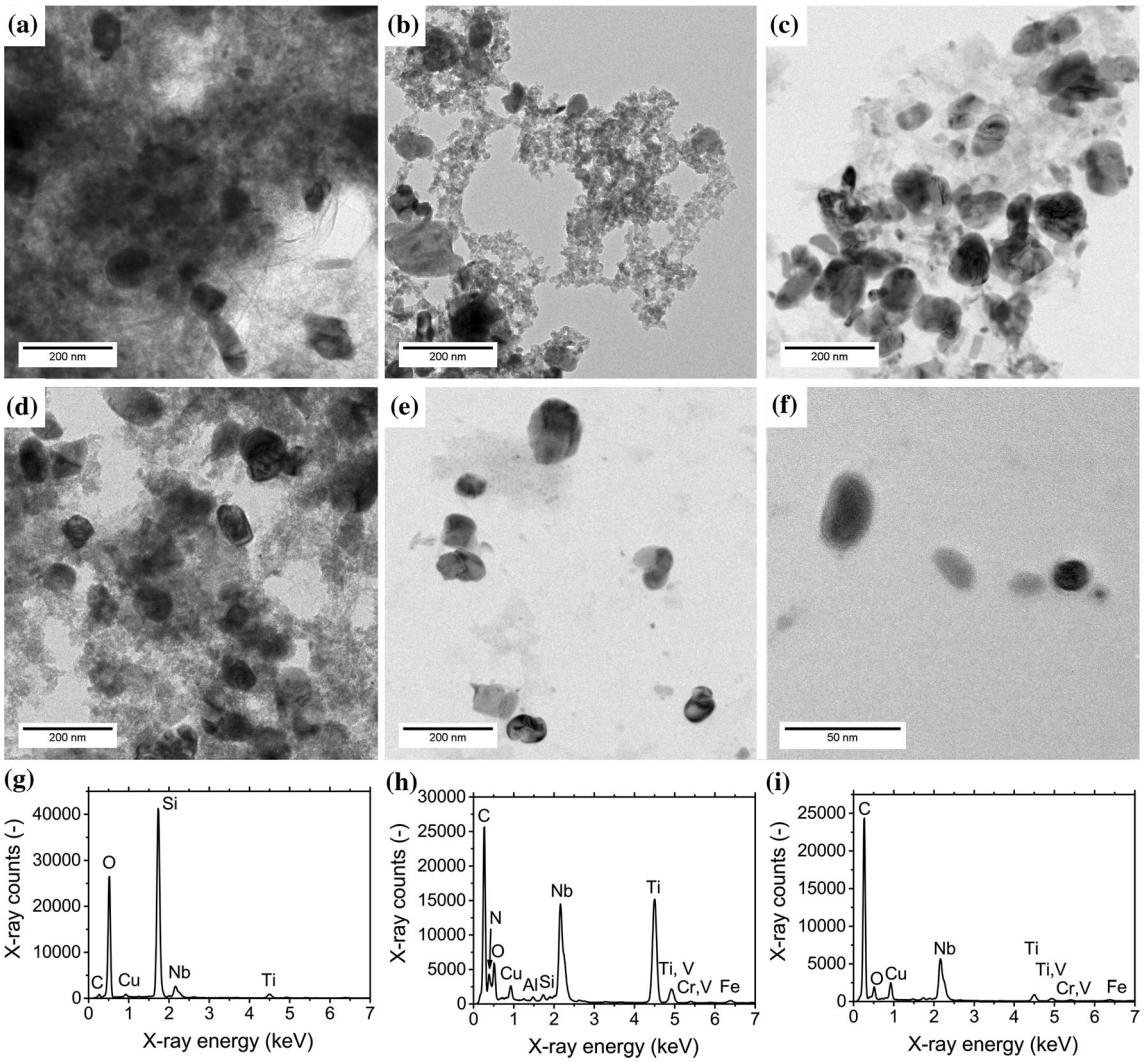

Figure 4 Transmission electron micrographs of particles extracted using **a** the ASTM standard, **b** 6 mol L^{-1} hydrochloric acid, **c** 2 mol L^{-1} H_2SO_4, **d** 0.5 mol L^{-1} H_2SO_4, **e** and **f** 0.5 mol L^{-1} H_2SO_4 with 0.1 vol% Disperbyk-2012. **g** Energy-dispersive X-ray spectrum recorded at the position of panel **a**. A strong Si signal is apparent. **h** and **i** EDX spectra of **e** and **f**. No Si is discernible. Note that the C and Cu signals originate from the TEM grid.

Discussion

Particle etching

The results clearly indicate unwanted etching of particles in all extraction protocols. Even optimized protocols caused losses of at least 6% of Nb and 9% of Ti that need to be considered in the interpretation of the results.

Several reasons allow us to exclude the alternative explanation that Ti or Nb was dissolved from solid solution in the steel. First, the steel samples used here were treated with a temperature ramp during TMCP that is likely to cause complete or almost complete precipitation of Ti and Nb as carbonitrides within the errors of the available thermodynamic data, so that the amount of Nb and Ti remaining as solid solution must be small. In addition, it was found that the amount of dissolved Ti and Nb for the same steel strongly depended on the acid type and etchant volume, even though all iron was dissolved in all cases: HCl led to lower concentrations than H_2SO_4, and larger etchant volumes strongly increased the concentration for both elements. The amount of dissolved Nb additionally depended on temperature and acid concentration that are very unlikely to affect the removal from solid solution. We are forced to

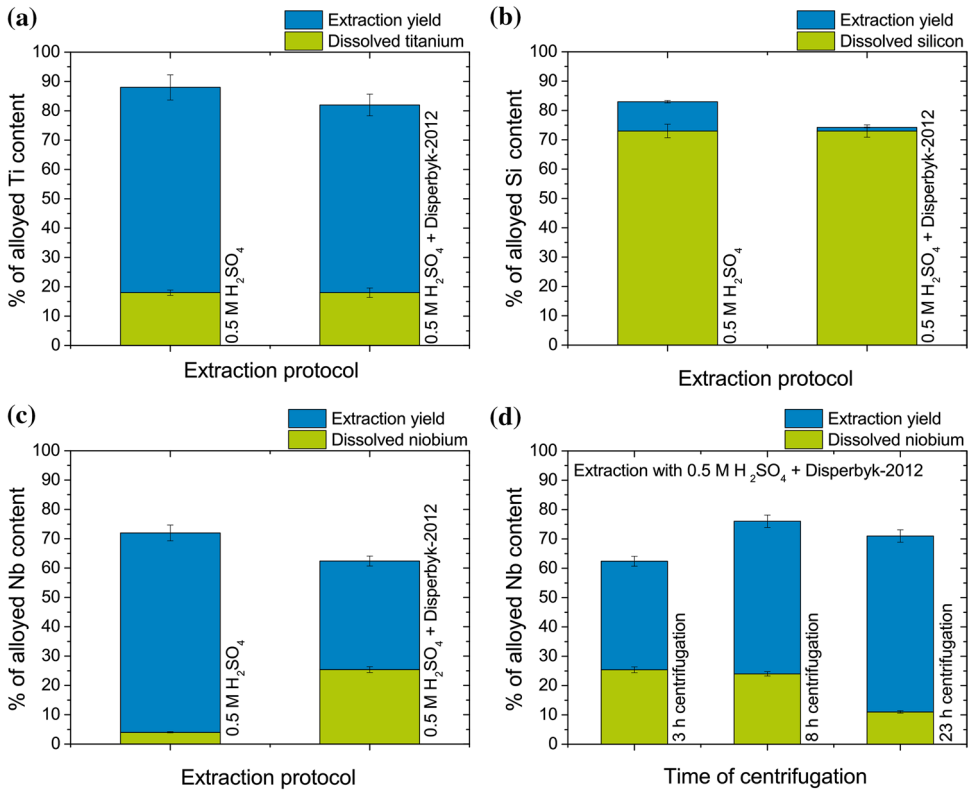

Figure 5 Amounts of titanium **a**, silicon **b**, and niobium **c** in the supernatant (green) and the residue (blue) after particle extraction with 0.5 mol L^{-1} H_2SO_4 and 0.5 mol L^{-1} H_2SO_4 with 0.1 vol% Disperbyk-2012. **d** Shows the influence of different centrifugation duration on the Nb content in the supernatant and extraction residue after particle extraction with 0.5 mol L^{-1} H_2SO_4 and 0.1 vol% Disperbyk-2012.

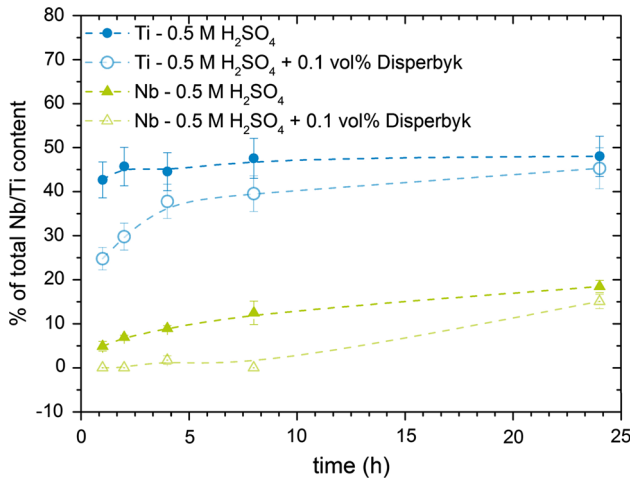

Figure 6 Time-dependent dissolution of NbCN and TiCN reference particles in 0.5 M H_2SO_4 and 0.5 M H_2SO_4 with 0.1 vol% Disperbyk-2012.

conclude that the particles were attacked by the etchants.

Experiments with reference particles support this interpretation. Higher acid concentration, higher temperatures, and higher etchant volumes led to increased particle etching. Interestingly, the experiments indicate that Ti and Nb concentrations in the supernatant rapidly increased in the first hours of the experiments and then reached saturation. Note that the reference particles experience a "worst case scenario" were all the acid only attacks the reference particles during the entire experiment, while acid is consumed in iron dissolution in the real extraction, and the losses from particles in steels are expected (and found) to be somewhat smaller.

The processes during extraction are complex, and there are several mechanisms that will require further studies until their role is fully understood. For example, the amount of Ti in the supernatant after 6 mol L^{-1} HCl extraction at 70 °C was surprisingly low. It was never possible to recover all Ti and Nb from the combined supernatant and residue, probably due to particle losses during the centrifugation process through adsorption on the walls of the centrifuge tubes or the glass beaker used for particle extraction. The smallest particles in steel have sizes of only a few nanometers and may well remain in the supernatant, where they are found by elementary analysis and indicate more extensive etching than actually took place. SiO_x network formation may reduce particle dissolution by engulfing the particles, separating them from the acid, and protecting them

from dissolution. On the other hand, even very small particles trapped in the SiO_x network sediment rather rapidly (a process that is exploited in commercial water purification with iron hydroxide networks, for example [38]), which may remove them from the supernatant and explain the good extraction yields of the ASTM protocol despite of its considerable etching. Finally, one would not expect that the particles are uniformly etched independent on their size; smaller particles may be etched faster than large particles. If very small particles with sizes (< 10 nm) are rapidly etched, the measured PSD of the extracted particles may be shifted toward larger sizes.

SiO_x network formation

The particles in Fig. 4 are embedded in a SiO_x network that impedes both electron microscopy, where the contrast is reduced and EDX suffers from a large silicon background, and colloidal particle analysis, where network fragments will be analyzed rather than the actual particles. The extent of network formation was quantified by comparing the amount of silicon in the supernatant (where it can be easily removed) and in the residue (where it forms networks). The ASTM protocol consistently led to much more silicon in the residue than in the supernatant, probably due to the long dissolution time that is sufficient for dense network formation. Shorter protocols considerably reduced the amount of silicon in the residue, thus facilitating later analysis.

The etchant volume and thus the concentration of silicon during dissolution were second important parameters to reduce the extent of silicon oxide network formation. We therefore recommend using moderately concentrated acids (to limit particle etching) in adequate volumes that suppress SiO_x formation but are not too high to exacerbate particle loss.

Not all silicon contained in the dissolved steels was found in the combined supernatant and residue, probably due to adsorption of SiO_x at the walls of glass containers. Teflon reduced this loss, but it led to the adsorption and loss of Nb and Ti-carbonitride particles. We recommend using protocols that inherently suppress SiO_x network formation.

Dispersant

We are not aware of any reported protocols for particle extraction with surfactants and performed extensive tests that led to markedly improved extraction result, with reduced agglomeration and silicon oxide network formation compared to the surfactant-free etchants. Experiments with reference particles indicate some protection of the particles from etching. The commercial dispersant that was used is based on block copolymers with groups designed to bind to the particle surfaces, thus forming a polymer shell that protects individual particles and stabilizes dispersion. The shell increased the hydrodynamic diameter, which needs to be considered for colloidal analysis, but it is readily penetrated by electrons and aids electron microscopy by spacing particles.

EDX analysis confirmed again that only Nb and Ti precipitated as carbides, nitrides, or carbonitrides. There may be traces of V present, but the K_β-peak of Ti is close to the K_α-line of V, the K_β-line of V is close to the K_α-line of Cr, and the overall peak is small. The TEM sample holder contains Cr, which is commonly found in traces. Simulations performed using Matcalc (see supplementary information) suggest that for the steel at hand, V-containing precipitates should occur less than 10^{-6} times the number of NbC precipitates. The traces of Fe in the residue are probably due to incomplete removal of the dissolved matrix; Cu is likely from the TEM grid. Carbon was ubiquitous and may originate from the particles or the amorphous carbon coating of the TEM grids. Nitrogen was only found for large particles. Most small particles appear to be pure carbides, a result that will be further investigated using other analysis techniques in forthcoming publications.

The reduction in silicon oxide network formation is probably due to the stabilization of the SiO_x sol that does not gel when stabilized by the dispersant. It is conceivable that the surfactant also slows down growth and leads to smaller SiO_x particles that are easily removed with the supernatant because of their small size and low density.

A surprising result is the increased content of Nb in the supernatant when introducing a surfactant. Part of this increase is most likely due to very small particles (with diameters in the single-nanometer range) that are stabilized by the surfactant, remain in the supernatant, and do not sediment during

centrifugation. Such small particles have rarely been addressed in extraction so far. Prolonging the centrifugation time increased recovery, but the amount of Nb in the supernatant after particle extraction without dispersant was still not reached. Dissolved Nb may enter the silicate network that is partially formed during extraction without dispersant. This could lower the amount of Nb found in the supernatant.

Titanium concentrations in the supernatant were much less affected by the dispersant. Most particles containing Ti particles are large (> 50 nm) and easily sediment during centrifugation.

Conclusion

The choice of protocol for particle extraction from microalloyed steel was found to be critical for reliable measurements. There exists a trade-off between particle loss by unwanted etching, the rate of steel dissolution, and the degree of SiO_x network formation. Higher acid concentrations and higher temperatures sped up extraction and reduced the formation of SiO_x networks but also increased particle etching. Even the best protocols caused a considerable loss of the particles, and it is conclusively shown that it is due to etching of the particles. This causes a reduction in the true particle diameter[2] on the order of 5% that should be reported when using such methods. Note that the uncertainties in size determination with electron microscopy depend on the image resolution and cause typical errors[3] on the order of 1–2% [17].

We introduced an improved extraction protocol that is based on 0.5 mol L^{-1} H_2SO_4 with 0.1 vol% Disperbyk-2012 as dispersant and a dissolution temperature of 70 °C. It reduced particle etching to 11% for Nb and 18% for Ti. A centrifugation time above 20 h (at the given rcf) is recommended to remove most of the smallest particles from the extraction suspension.

Addition of a surfactant improved the extraction results by stabilizing the particles without decreasing the extraction yield, and we recommend the use of suitable surface agents in particular when colloidal analysis of the extracted particles is intended. There are indications that the surfactants stabilize even very small particles with diameters below 10 nm, making them accessible to characterization techniques beyond electron microscopy.

[2] $V \sim r^3$: a reduction of 15% in volume/mass goes along with a reduction of approx. 5% in radius.

[3] For an image resolution with 2 pixels/nm and a particle size of 30 nm, the error in size determination is 1.6%.

Acknowledgements

The authors would like to thank Eduard Arzt for his continuing support of the project. Andrea Jung is also acknowledged for the elementary analysis, Kathrin Alt for particle dissolution experiments, and Bastian Philippi for Matcalc Simulations.

Funding

This work was funded by the "AG der Dillinger Hüttenwerke" in Germany and a patent for a particle extraction procedure aided by a dispersant was submitted.

Electronic supplementary material: The online version of this article (https://doi.org/10.1007/s10853-018-03263-0) contains supplementary material, which is available to authorized users.

References

[1] Vega MI, Medina SF, Quispe A et al (2005) Influence of TiN particle precipitation state on static recrystallisation in structural steels. ISIJ Int 45:1878–1886. https://doi.org/10.2355/45.1878

[2] Nishioka K, Ichikawa K (2012) Progress in thermomechanical control of steel plates and their commercialization. Sci Technol Adv Mater 13:023001. https://doi.org/10.1088/1468-6996/13/2/023001

[3] Baker TN (2016) Microalloyed steels. Ironmak Steelmak 43:264–307. https://doi.org/10.1179/1743281215Y.0000000063

[4] Gladman T (1997) The physical metallurgy of microalloyed steels. The Institute of Materials, London

[5] Craven AJ, He K, Garvie LAJ, Baker TN (2000) Complex heterogeneous precipitation in titanium–niobium microalloyed Al-killed HSLA steels—I. (Ti, Nb)(C, N) particles. Acta Mater 48:3857–3868. https://doi.org/10.1016/S1359-6454(00)00194-4

[6] Craven AJ, He K, Garvie LAJ, Baker TN (2000) Complex heterogeneous precipitation in titanium–niobium

microalloyed Al-killed HSLA steels—II. Non-titanium based particles. Acta Mater 48:3869–3878. https://doi.org/10.1016/S1359-6454(00)00193-2

[7] Courtois E, Epicier T, Scott C (2006) EELS study of niobium carbo-nitride nano-precipitates in ferrite. Micron 37:492–502. https://doi.org/10.1016/j.micron.2005.10.009

[8] Lee Y, De Cooman BC (2014) TiN/NbC compound particle formation during thin slab direct rolling of HSLA steel. Steel Res Int 85:1158–1172. https://doi.org/10.1002/srin.201300280

[9] Xie ZJ, Ma XP, Shang CJ et al (2015) Nano-sized precipitation and properties of a low carbon niobium micro-alloyed bainitic steel. Mater Sci Eng A 641:37–44. https://doi.org/10.1016/j.msea.2015.05.101

[10] Li Z, Liu D, Zhang J, Tian W (2013) Precipitates in Nb and Nb–V microalloyed X80 pipeline steel. Microsc Microanal 19:62–65. https://doi.org/10.1017/S1431927613012348

[11] Béreš M, Weirich TE, Hulka K, Mayer J (2004) TEM investigations of fine niobium precipitates in HSLA steel. Steel Res Int 75:753–758

[12] Klinkenberg C, Hulka K, Bleck W (2004) Niobium carbide precipitation in microalloyed steel. Steel Res Int 11:744–752

[13] Tirumalasetty GK, van Huis MA, Fang CM et al (2011) Characterization of NbC and (Nb, Ti)N nanoprecipitates in TRIP assisted multiphase steels. Acta Mater 59:7406–7415. https://doi.org/10.1016/j.actamat.2011.08.012

[14] Mukherjee T, Stumpf WE, Sellars CM (1968) Quantitative assessment of extraction replicas for particle analysis. J Mater Sci 3:127–135. https://doi.org/10.1007/BF00585479

[15] Shen YF, Wang CM, Sun X (2011) A micro-alloyed ferritic steel strengthened by nanoscale precipitates. Mater Sci Eng A 528:8150–8156. https://doi.org/10.1016/j.msea.2011.07.065

[16] Bonevich JE, Haller WK (2010) NIST—NCL joint assay protocol, PCC-X: measuring the size of nanoparticles using transmission electron microscopy (TEM). National Institute of Standards and Technology, Gaithersburg, MD. https://ws680.nist.gov/publication/get_pdf.cfm?pub_id=854083. Accessed 19 Dec 2018

[17] Rice SB, Chan C, Brown SC et al (2013) Particle size distributions by transmission electron microscopy: an interlaboratory comparison case study. Metrologia 50:663–678. https://doi.org/10.1088/0026-1394/50/6/663

[18] Masuda H, Gotoh K (1999) Study on the sample size required for the estimation of mean particle diameter. Adv Powder Technol 10:159–173. https://doi.org/10.1016/S0921-8831(08)60447-1

[19] Cunningham TR, Price RJ (1933) Determination of non-metallic inclusions in plain carbon and manganese steels iodine and nitric acid extraction methods. Ind Eng Chem Anal Ed 5:27–29. https://doi.org/10.1021/ac50081a018

[20] Klinger P, Koch W (1938) Beitrag zur elektrolytischen Bestimmung von nichtmetallischen Einschlüssen im Stahl. Arch für das Eisenhüttenwes 11:569–582. https://doi.org/10.1002/srin.193801061

[21] Inoue R, Ueda S, Ariyama T, Suito H (2011) Extraction of nonmetallic inclusion particles containing MgO from steel. ISIJ Int 51:2050–2055

[22] Garside JE, Rooney TE, Belli JJJ (1957) The alcoholic-iodine method for the extraction of inclusions from steel. J Iron Steel Inst 185:95–103

[23] Fernandes M, Cheung N, Garcia A (2002) Investigation of nonmetallic inclusions in continuously cast carbon steel by dissolution of the ferritic matrix. Mater Charact 48:255–261. https://doi.org/10.1016/S1044-5803(02)00246-2

[24] Lu J, Ivey D, Henein H (2006) Quantification of nano-sized precipitates in microalloyed steels by matrix dissolution. In: Proceedings of international pipeline conference, pp 635–642. https://doi.org/10.1115/ipc2006-10600

[25] Lu J, Ivey DG, Henein H et al (2008) Extraction and characterization of nano-precipitates in microalloyed steels. In: Proceedings of the international pipeline conference, Calgary, pp 85–94

[26] Lu J, Wiskel JB, Omotoso O et al (2011) Matrix dissolution techniques applied to extract and quantify precipitates from a microalloyed steel. Metall Mater Trans A 42:1767–1784. https://doi.org/10.1007/s11661-010-0579-6

[27] Hegetschweiler A, Kraus T, Staudt T (2017) Colloidal analysis of particles extracted from microalloyed steel. Metall Ital 109:23–28

[28] Wiskel J, Lu J, Omotoso O et al (2016) Characterization of precipitates in a microalloyed steel using quantitative X-ray diffraction. Metals (Basel) 6:90. https://doi.org/10.3390/met6040090

[29] Rivas AL, Vidal E, Matlock DK, Speer JG (2008) Electrochemical extraction of microalloy carbides in Nb-steel. Rev Metal 44:447–456. https://doi.org/10.3989/revmetalm.0771

[30] ASTM E194-10 (2015) Standard test method for acid-insoluble content of copper and iron powders, West Conshohocken

[31] Pierson HO (1996) Carbides of group IV: titanium, zirconium, and hafnium carbides. In: Pierson HO (ed) Handbook of refractory carbides and nitrides: properties, characteristics, processing and applications. Noyes Publications, Westwood, p 362

[32] Pierson HO (1996) Carbides of group V: vanadium, niobium and tantalum carbides. In: Pierson HO (ed) Handbook of refractory carbides and nitrides: properties, characteristics,

processing and applications. Noyes Publications, Westwood, p 362

[33] Pierson HO (1996) The refractory nitrides. In: Pierson HO (ed) Handbook of refractory carbides and nitrides. Noyes Publications, Westwood, pp 156–162

[34] Kosolapova TY (2012) Carbides. Springer, Boston

[35] Lengauer W (2000) Transition metal carbides, nitrides, and carbonitrides. In: Riedel R (ed) Handbook of ceramic hard materials. Wiley, Weinheim, pp 202–252

[36] Giordano C, Erpen C, Yao W et al (2009) Metal nitride and metal carbide nanoparticles by a soft urea pathway. Chem Mater 21:5136–5144. https://doi.org/10.1021/cm9018953

[37] Read S, Gibbs R, Parker B (1990) Extraction and characterization of precipitates formed in a niobium HSLA steel. Mater Forum 14:304–307

[38] Duan J, Gregory J (2003) Coagulation by hydrolysing metal salts. Adv Colloid Interface Sci 100–102:475–502. https://doi.org/10.1016/S0001-8686(02)00067-2